

Non-equilibrium electronic transport and interaction in short metallic nanobridges

H. B. Weber^{1†}, R. Häussler¹, H. v. Löhneysen^{1,2}

¹ *Physikalisches Institut, Universität Karlsruhe, D-76128 Karlsruhe*

² *Forschungszentrum Karlsruhe, Institut für Nanotechnologie, D-76021 Karlsruhe*

J. Kroha

Institut für Theorie der Kondensierten Materie, Universität Karlsruhe, D-76128 Karlsruhe

(September 13, 2018)

We have observed interaction effects in the differential conductance G of short, disordered metal bridges in a well-controlled non-equilibrium situation, where the distribution function has a double Fermi step. A logarithmic scaling law is found both for the temperature and for the voltage dependence of G in all samples. The absence of magnetic field dependence and the low dimensionality of our samples allow us to distinguish between several possible interaction effects, proposed recently in nanoscopic samples. The universal scaling curve is explained quantitatively by the theory of electron-electron interaction in diffusive metals, adapted to the present case, where the sample size is smaller than the thermal diffusion length.

Pacs numbers: 72.15.-v 72.80.Ng, 73.23.-b, 73.40.-c

I. INTRODUCTION

Dynamically screened electron-electron interactions in disordered metals are known to cause singular corrections to the electronic density of states (DOS), as explained by Aronov and Al'tshuler^{1,2}. The corresponding zero-bias anomalies (ZBA) have been studied by tunneling spectroscopy on wide junctions in thermodynamic equilibrium^{3,4}. How is the ZBA modified when a large current is driven through the system by a finite bias voltage, and the bridge is so small that there is phase coherence across the whole sample? In this case, no local equilibrium is reached, since energy relaxation does not occur within the sample. Instead, the distribution function of electrons traversing the system exhibits two Fermi steps related to the two different electrochemical potentials of the two leads. This fact has been claimed theoretically^{5,6} and has recently been confirmed in tunneling experiments⁷ (where in addition the steps were rounded due to interactions in long wires) and indirectly by noise measurements in a similar setup⁸.

We have fabricated metallic nanobridges, which allow for the first time to study the Aronov-Al'tshuler anomaly¹ in the stationary non-equilibrium situation specified above. A two-dimensional (2D), diffusive metal bridge, much shorter than all inelastic scattering lengths, is placed in good metallic contact between two thick reservoirs. A high lead-to-bridge aspect ratio allows to maintain a finite voltage drop across the bridge despite its small resistance, thus allowing the observation of temperature-voltage scaling behavior. The study of a 2D bridge is further motivated by the fact that this geometry allows to distinguish between the Aronov-Al'tshuler conductance anomaly and a possible two-channel Kondo effect induced by two-level systems⁹, which has been put forward as the origin of ZBAs observed in ultrasmall point contacts¹⁰. In 3D both the

Aronov-Al'tshuler and the two-channel Kondo anomalies show square root power-law behavior; in 2D the Aronov-Al'tshuler correction is logarithmic, while the two-channel Kondo singularity, as a local effect, is independent of dimension. As will be discussed, the conductance through the non-equilibrium bridge can be well described by a two-terminal Landauer-Büttiker formula, generalized for interacting systems¹¹. Applying the theory of electron-electron interaction in disordered systems in non-equilibrium, we find that the electronic DOS is strongly modified by the non-equilibrium and displays two logarithmic singularities, corresponding to the two steps in the distribution function. This yields quantitative agreement with the experimental results.

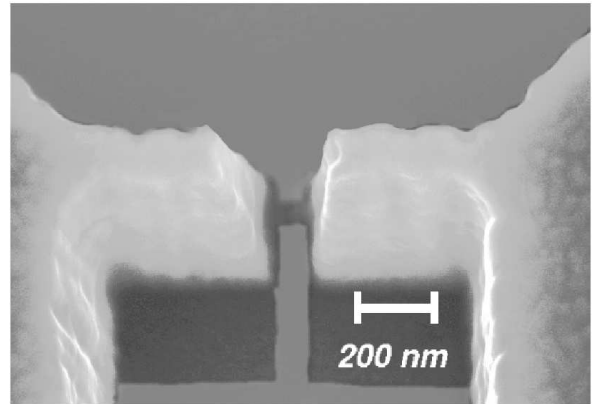


FIG. 1. SEM picture of one of the samples, which were produced by the shadow-evaporation technique. The thin $\text{Cu}_{82}\text{Au}_{18}$ bridge (dark) is embedded between two considerably thicker Cu leads. Dark regions are the thin shadow-evaporation replicas of the thick leads. A thick replica of the bridge, which is not connected to the electrodes, is removed from the picture for clarity.

II. EXPERIMENT

The samples were produced by the shadow-evaporation technique¹². Metal was deposited at two different angles under UHV conditions through a PMMA mask patterned with e-beam lithography. We deposited 10 nm of $\text{Cu}_{100-x}\text{Au}_x$ for the bridge at one angle (-13° off the normal direction of the surface) and 700 nm of Cu for the reservoirs ($+13^\circ$) at the opposite angle without breaking the vacuum (on the 10^{-9} mbar scale during evaporation). The transport measurements were performed in a $^3\text{He}/^4\text{He}$ dilution refrigerator in a temperature range between $T = 100$ mK and $T = 2.1$ K. The differential resistance was measured with a LR 700 resistance bridge, which was capacitively coupled to a DC circuit through the sample. The AC excitation was less than $5 \mu\text{V}$.

| No. | | d [nm] | R [Ω] | D [cm^2/s] | ℓ [nm] | $A_{B=0\text{T}}$ [e^2/h] | $A_{B=8.5\text{T}}$ [e^2/h] |
|-----|--------------------------------|-------------|---------------------|-----------------------------------|----------------|----------------------------------|------------------------------------|
| 1 | $\text{Cu}_{82}\text{Au}_{18}$ | 10 | 13.6 | 34 | 6.5 | 0.49 | 0.48 |
| 2 | $\text{Cu}_{82}\text{Au}_{18}$ | 10 | 16 | 31 | 6.0 | 0.51 | – |
| 3 | $\text{Cu}_{50}\text{Au}_{50}$ | 20 | 6.5 | 37 | 7.0 | 0.42 | 0.45 |
| 4 | Cu | 10 | 5.5 | 68 | 13 | 0.7 | 0.43 |

TABLE I. Characteristic parameters for the four investigated nanobridges: material composition, thickness d , resistance R , diffusion coefficient D , mean free path ℓ , and the amplitude A of the zero-bias anomaly at an applied magnetic field of $B = 0$ and $B = 8.5$ T, respectively (see text). In high magnetic field the pure Cu sample exhibits the same ZBA as all other samples, but in low field shows an enhanced amplitude of the effect, while the scaling behavior Eqs. (1), (2) remains valid. This needs further investigation.

The parameters characterizing the four different samples investigated in this study are summarized in table I. Each of the four nanobridges is $L = 80$ nm long, about 80 nm wide and their thickness d is substantially smaller than the lateral extension L . It is placed in good metallic contact between two bulk Cu leads, which are about 70 times thicker than the bridge and extend over a large area of about 1 mm^2 each (see Fig. 1). Hence the voltage applied to the sample drops only along the bridge, and the arising heating power is reliably conducted away by the leads. This was verified in a control experiment, where the cooling capability of the reservoirs was varied using a different geometry. No change of the behavior reported below was observed. Moreover, as demonstrated in detail below, the electronic motion is coherent over the entire size of the nanobridge, which means, in particular, that there is no heat deposition within the bridge. The elastic mean free path ℓ was estimated from the residual-resistance ratio and consistently from the Drude formula. In all samples ℓ is comparable to the thickness d , but much shorter than the lateral length L , and therefore, the electronic density modes in the bridge obey the rules of 2D diffusive motion. Below we present experimental

conductance data of sample no. (1); the results obtained from the other $\text{Cu}_{100-x}\text{Au}_x$ and Cu films are very similar.

Raw data of the zero-bias conductance as a function of temperature T are shown in Fig. 2. We observe a logarithmic T dependence between $T = 100$ mK and $T = 2$ K:

$$G(0, T) = G(0, T_o = 1\text{K}) + A \cdot \ln(T/T_o), \quad (1)$$

where A denotes the amplitude of the effect, with $A = 0.49 e^2/h$ for this particular bridge. Below $T = 100$ mK, small deviations from the form Eq. (1) were observed, which are probably due to incomplete thermalization of the sample at the lowest temperatures. Such logarithmic behavior has often been observed in thin metallic films and metallic nanobridges and is usually attributed to weak localization¹³ and/or electron-electron interaction¹.

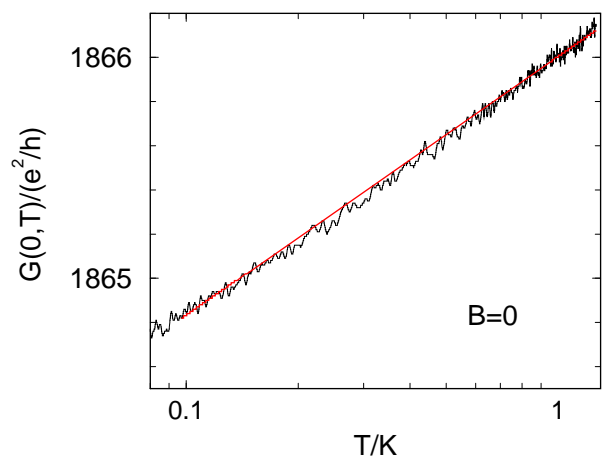


FIG. 2. Zero-bias conductance of the $\text{Cu}_{82}\text{Au}_{18}$ bridge. The straight line is a fit according to Eq. (1).

When applying a bias voltage U , small deviations from Ohmic behavior, i.e. a voltage-dependent differential conductance $G = dI(U)/dU$, are observed at low U , as shown in Fig. 3. This zero-bias anomaly (ZBA), symmetrical with respect to reversal of U , becomes continuously more pronounced as T is lowered. For all voltage sweeps taken for various T in the range of 0.1 K to 2.1 K, one observes a remarkable scaling property: If one subtracts the zero-bias conductance of each sweep and plots $G(U, T) - G(0, T)$ as a function of U/T , all conductance sweeps collapse onto a single curve, as can be seen in Fig. 3. Comparison with results of several $\text{Cu}_{100-x}\text{Au}_x$ samples and for pure Cu samples (with a mean free path comparable to the thickness of the wire) yields a further general property $(G(U, T) - G(0, T))/A$ is identical for all samples (table I), where A is the zero-bias anomaly amplitude defined above. We therefore propose the following scaling law:

$$\frac{G(U, T) - G(0, T)}{A} \equiv \Phi(eU/k_B T) \quad (2)$$

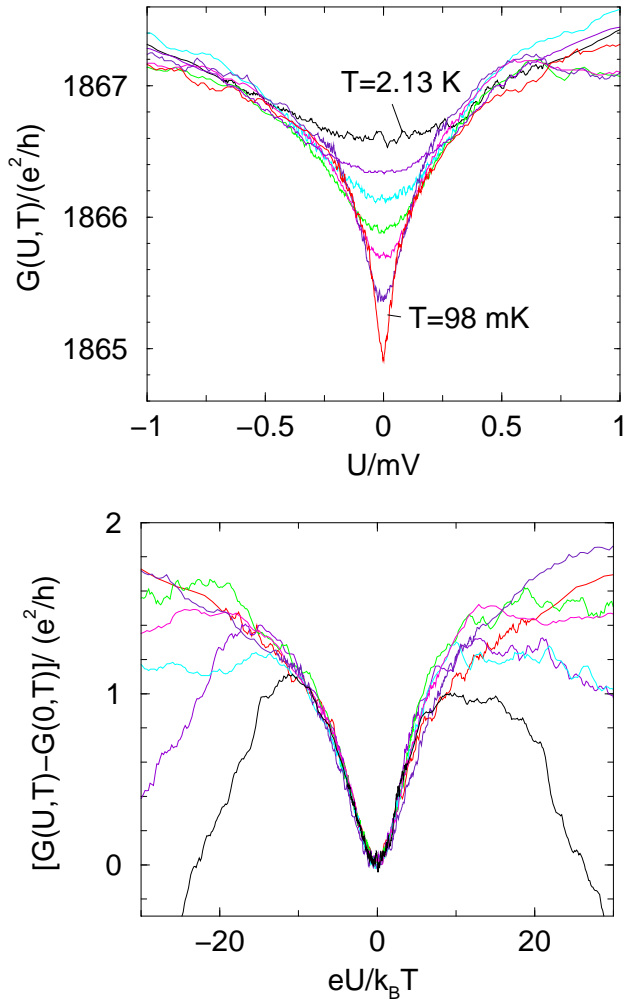


FIG. 3. Top: Raw data of the voltage dependence of the differential conductance for different temperatures: $T=0.1$ K, 0.25 K, 0.5 K, 0.75 K, 1 K, 1.5 K, 2.1 K. Bottom: The scaling of the same data appears, when the zero-bias conductance is subtracted from each curve and the data are displayed as a function of $eU/k_B T$.

where Φ is a function of $eU/k_B T$ only. Other scaling laws, in particular \sqrt{T} dependence as expected for the two-channel Kondo effect¹⁰, fit very poorly to the data. Fig. 4 shows the function Φ extracted from conductivity measurements on one sample at seven different temperatures as a function of $y = eU/k_B T$ on a semi-logarithmic scale (data of positive and negative bias are included). Within some scatter due to experimental noise, all sweeps collapse onto one single curve. At $|y| < 1$, the conductance is essentially constant, which corresponds to thermal smearing. At $|y| > 1$, the behavior is roughly logarithmic, and for still larger values of $|y|$, the curves deviate from scaling. The low- T data follow the logarithmic behavior up to $y \simeq 100$, while the high- T data deviate at lower y . These deviations at higher energies are attributed to heating effects and/or additional high-energy processes like phonon excitations

and are well known from similar experiments¹⁰.

When a perpendicular magnetic field of up to $B = 8.5T$ is applied, we do not observe any systematic change of the conductance behavior apart from universal conductance fluctuations (UCF). In particular, the scaling behavior persists, with the amplitude A and the scaling function Φ remaining unchanged. We expect a weak localization conductance correction of $\delta G_{WL}(U = 0, T = 0, B = 0) \approx 3.2e^2/h$, which is not clearly distinguishable from the UCFs in our small samples. However, the fact that the amplitude A of the ZBA as a function of applied voltage U (i.e. the slope of the logarithmic scaling curve) remains unchanged in a magnetic field of $B = 8.5T$ indicates that weak localization only gives a constant, voltage independent correction and that the logarithmic increase of the conductance with applied voltage is not due to a loss of coherence at finite voltage and a subsequent suppression of weak localization, since otherwise the effect would disappear in a magnetic field. This, in turn, provides clear evidence that the samples are coherent even at finite bias voltage U as expected from their small size.

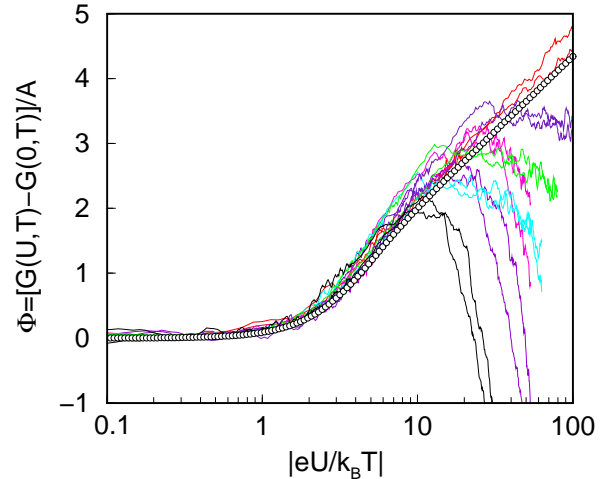


FIG. 4. Logarithmic scaling plot according to Eq. (2) for the data presented in Fig. 3. Lines represent experimental data for various fixed T . Circles represent the theoretical scaling curve computed from Eqs. (6), (10), (3).

Logarithmic behavior may also be caused by magnetic impurities or by non-magnetic two-channel Kondo defects⁹ above their respective Kondo temperatures T_K . Since an applied field of $B = 8.5$ T does not modify the ZBA, any magnetic impurities present in the sample must have $T_K \gg 8.5$ K. However, the logarithmic behavior of the zero-bias conductance observed down to the lowest T (Fig. 2) puts an upper bound to the Kondo temperature, $T_K < 0.1$ K, thus ruling out magnetic impurities as the origin of the ZBA. In the two-channel Kondo scenario, from point-contact spectroscopy on Cu one expects $T_K \approx 5$ to 10 K^{10,14}. Hence, it is unlikely that the ZBA is due to two-channel Kondo defects for the same reason

as in the magnetic case. The assumption that there is no sizable number of two-channel Kondo defects present in our $\text{Cu}_{82}\text{Au}_{18}$ samples is consistent with the fact that in previous Cu point contacts the two-channel Kondo signal completely disappeared upon doping with 1% Au or more¹⁰.

III. THEORY

In the following we show that the observed scaling behavior of the differential conductance can be explained quantitatively by electron-electron interaction within a model calculation for the non-equilibrium DC transport through our small, disordered metal bridges. Since the diffusion time of an electron through the bridge, $\tau_D = L^2/D \approx 1.8$ ps, is short compared to the dephasing time τ_φ and the energy relaxation time τ_i , the electrons occupy the exact eigenstates of the disordered bridge while traversing the system. Therefore, the DC transport is coherent (zero-dimensional), even when a finite bias voltage is applied as discussed above, i.e. the interacting eigenstates of the bridge serve as transmission channels. In such a situation a generalized Landauer-Büttiker approach can be applied, where the conductance is expressed in terms of the interacting, non-equilibrium DOS $\mathcal{N}(\omega)$ of the bridge in the presence of coupling to the leads¹¹. Diffusive density modes, which exist at time scales down to the elastic scattering time $\tau = \ell/v_F \approx 4.1$ fs $\ll \tau_D$ couple to the electronic DOS via the dynamically screened Coulomb interaction and thus give a singular correction to the conductance as shown below.

Because of the good metallic contact, charging effects at the interfaces¹⁵ are negligible in our devices. Since the transition between the reservoirs and the bridge occurs abruptly on a scale small compared to the extension of the bridge wave functions and energy relaxation in the bridge is negligible, one may represent the system in terms of the exact eigenstates $|n\sigma\rangle$ of the bridge, separated from the leads, and include the bridge-lead coupling to infinite order in perturbation theory^{16,11} (assumed to be convergent). Denoting the corresponding creation operators for eigenstates with spin σ in the left (right) leads and the bridge by $a_{L(R)k\sigma}^\dagger$, $c_{n\sigma}^\dagger$, respectively, the hamiltonian of the device is $H = H_L + H_R + H_B + H_V$. Here, $H_{L(R)} = \sum_k \varepsilon_k a_{L(R)k\sigma}^\dagger a_{L(R)k\sigma}$ are the left (right) lead hamiltonians with spectral density $A_{k\sigma}(\omega)$ and a flat bulk DOS $N_o = \sum_{k\sigma} A_{k\sigma}(\omega)$. $H_V = \sum_{kn\sigma} [V_{nk}^L c_{n\sigma}^\dagger a_{Lk\sigma} + V_{nk}^R c_{n\sigma}^\dagger a_{Rk\sigma}] + h.c.$ describes mixing between bridge and leads via transition matrix elements $V_{nk}^{L(R)}$, and H_B is the hamiltonian of the bridge, including random impurity scattering and Coulomb interaction. For later use we also introduce the effective couplings $\Gamma_{\sigma mn}^{L(R)}(\omega) = 2\pi \sum_k V_{mk}^{L(R)} A_{k\sigma}(\omega) V_{kn}^{L(R)*} \equiv \Gamma^{L(R)}$, and $\Gamma = \Gamma^L \Gamma^R / (\Gamma^L + \Gamma^R)$, which will be assumed to be independent of energy and of the channels

m, n of the bridge.

Using the Dyson equation for the Keldysh matrix Green function $\widehat{\mathcal{G}}_{n\sigma}(\omega)$ in terms of the exact eigenstates of the bridge, it is straight-forward to show that at finite bias and for negligible energy relaxation the distribution function $f(\omega)$ of quasiparticles is a linear superposition of the distribution functions in the leads,

$$f(E) = \frac{1}{\Gamma^L + \Gamma^R} [\Gamma^L f^{(0)}(E) + \Gamma^R f^{(0)}(E + eU)], \quad (3)$$

where $f^o(E) = 1/(e^{E/k_B T} + 1)$ is the Fermi function. The distribution function $f(E)$, Eq. (3), represents the probability for eigenstates of the entire bridge with energy E being occupied and, therefore, is position independent. It should be emphasized that this is to be distinguished from the local distribution function $f_x(E)$, which is defined as the probability of finding an electron in a state with energy E within a small volume centered at position x wherein the externally applied fields are slowly varying¹⁷. When, as in the present case, the interaction correction to the local DOS is small ($\delta\mathcal{N}_x(E)/\mathcal{N}_x(E) \ll 1$), in a disordered system $f_x(E)$ obeys a diffusive kinetic equation^{6,18}

$$-D\nabla^2 f_x(E) = C(\{f_x\}, x, E). \quad (4)$$

For negligible energy relaxation the collision integral C vanishes, and $f_x(E)$ is a linear superposition of Fermi functions $f^{(0)}(E)$, $f^{(0)}(E + eU/\hbar)$ with coefficients depending linearly on the position x along the bridge. It follows directly from the definitions of $f(E)$ and $f_x(E)$ via the total and the local density matrices, respectively, that

$$f(E) = \int_0^L \frac{dx}{L} f_x(E) \quad (5)$$

The local distribution $f_x(E)$ has been measured in tunneling experiments of Ref. [7], while for the description of the present experiment only the integrated distribution $f(E)$, Eq. (3), is needed.

An exact, Landauer-Büttiker-like expression for the current $I(U)$ follows from the equation of motion of the reservoir electron density¹¹,

$$I = \frac{e}{\hbar} \int dE [f^o(E) - f^o(E + eU)] \Gamma \text{tr} [\text{Im} \mathcal{G}^r(E)], \quad (6)$$

where \mathcal{G}^r is the exact retarded single-particle Green function for the bridge in the presence of the leads, and the trace extends over the complete basis of bridge eigenstates, including spin. The problem of the DC current at arbitrary bias voltage is thus reduced to calculating the non-equilibrium DOS, $\mathcal{N}(E) = -\frac{1}{\pi} \text{tr} \text{Im} \mathcal{G}^r(E)$. Note that the diffusion constant D does not appear explicitly in Eq. (6), since the DC transport is zero-dimensional.

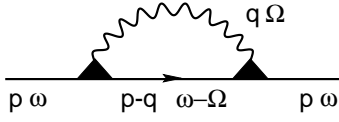


FIG. 5. Leading DOS correction. Solid lines: conduction electron Green functions; wavy line with solid triangles: dynamically screened Coulomb interaction \bar{v}_q .

The leading singular DOS correction due to dynamically screened Coulomb interaction² is shown diagrammatically in Fig. 5. It is seen that it is a *linear* functional of the quasiparticle distribution function $f(E)$. It may, therefore, be evaluated as a linear superposition of two *equilibrium* electron liquids with respective chemical potentials $\mu_L = 0$, $\mu_R = eU$, and by going over to the Matsubara representation. The trace involved in $\delta N(E)$ may be conveniently evaluated in a basis of momentum states \vec{p} . It reads $\text{tr} \delta \mathcal{G} = \text{tr}(\Gamma^L \delta \mathcal{G}^L + \Gamma^R \delta \mathcal{G}^R)/2\Gamma$, with (Fig. 5),

$$\text{tr} \delta \mathcal{G}^\alpha(iE) = \frac{2}{\beta} \sum_{p, q; \Omega > |E|} \bar{v}_q(i\Omega, iE) G_p^\alpha(iE)^2 G_{p-q}^\alpha(iE - i\Omega), \quad (7)$$

where $G_p^\alpha(i\omega) = 1/(iE + \mu_\alpha - \varepsilon_p + i/2\tau \text{sgn}E)$, $\alpha = L, R$ are the non-interacting Green functions. The dynamically screened Coulomb interaction in 2D, including vertex corrections, is¹

$$\bar{v}_q(Z, z) = \frac{-\frac{1}{\tau^2} v_q \Theta(-z''(z + Z)'')}{[Z \text{sgn}Z'' + iq^2 D][Z \text{sgn}Z'' + iv_q q^2 N_o D]} \quad (8)$$

with " denoting the imaginary part. In Eq.(8) there appears the Fourier transform of the bare Coulomb interaction in samples with finite thickness d , $v_q = (4e^2 d/q) \arctan(\pi/qd)$, which shows a crossover from 3D behavior at large wave numbers ($q > \pi/d$) to 2D behavior at small wave numbers ($q < \pi/d$). The inverse screening length in 2D is $\kappa = 2\pi e^2 N_o d$. According to our sample dimensions, $2\pi/k_F \ll \ell \lesssim d \ll L$, the quasiparticle momentum \vec{p} is integrated over the 3D momentum space, while the wave number of the diffusion mode is 2D and restricted to the range $2\pi/L < |\vec{q}| < 2\pi/\ell$. Thus we obtain the DOS correction

$$\delta \mathcal{N}(E) = \frac{1}{E_{Th}} \int_{-1/\tau}^{1/\tau} \frac{d\Omega}{2\pi^2} f(\Omega - E) \frac{1}{\Omega} \left[\pi \frac{d}{L} + \frac{1}{2} \ln \frac{\Omega^2 + (4\pi^2 E_{Th})^2}{\Omega^2 + (4\pi^2 D/\ell^2)^2} - \ln \frac{\Omega^2 + (2\pi\kappa D/L)^2}{\Omega^2 + (2\pi\kappa D/\ell)^2} \right], \quad (9)$$

where $E_{Th} = \hbar D/L^2 \approx 0.35$ meV is the Thouless energy. The first term in quare brackets originates from the $q = 0$ diffusion mode, which must be counted separately due to the discreteness of the allowed q values in the 2D sample of finite lateral size L . In the case of an infinite, 2D film ($L \rightarrow \infty$, $E_{Th} < k_B T$), this expression recovers the well-known DOS correction¹ $\delta \mathcal{N} \propto -\ln(E\tau/\hbar) \ln(E/\hbar\kappa^2 D)$.

For our finite-size bridges, however, the log divergence of the term in square brackets is cut off, and a single logarithmic singularity remains. Thus, we expect a crossover from \log^2 to simple log behavior in finite-size 2D films, as the energy considered becomes less than E_{Th} . Near the Fermi edges ($|E| \lesssim (2\pi)^2 E_{Th}$, $|E + eU| \lesssim (2\pi)^2 E_{Th}$) the logarithmic DOS correction may be cast into the form

$$\delta \mathcal{N}(y, u, T) = \frac{d/L}{2\pi E_{Th}} \times \left[\ln(T\tau) + \int d\varepsilon \left(-\frac{d\bar{f}(\varepsilon - y)}{d\varepsilon} \right) \ln|\varepsilon| \right], \quad (10)$$

where $\bar{f}(\varepsilon) = f(\Omega/k_B T)$ is the distribution function in terms of the dimensionless energy. $\delta \mathcal{N}(y, u, T)$ depends on two dimensionless energies, the quasiparticle energy $y = E/k_B T$ and the bias voltage $u = eU/k_B T$. At finite T it exhibits a logarithmic dip at each of the two Fermi edges at $y = 0$ and at $y = -eU/k_B T$, as shown in Fig. 6. The differential conductance correction $\delta G/A = [G(U, T) - G(0, T)]/A$, with $G(U, T) = dI/dU = d(I/k_B T)/du$, is calculated using Eqs. (6), (10) and (3), where the dimensionless quasiparticle energy $E/k_B T$ is integrated over, yielding a single-parameter scaling form in terms of $u = U/k_B T$. The resulting scaling curve does not contain any adjustable parameters and agrees quantitatively with the experimental data, as shown in Fig. 4. It is characteristic for log behavior that in Eq. (10), and consequently also in the conductance $G(U, T)$, the prefactor of the term depending on the dimensionless voltage u is independent of T and is equal to the amplitude of the T -dependent term $\ln(T\tau)$ at $y = 0$. This is in contrast to, e.g., power-law scaling or $\log^2(E/k_B T)$ dependence of the DOS correction and, hence, can be used to distinguish the latter behaviors from simple log scaling in the experimental data.

From the above discussion it is seen that the scaling of the non-linear conductance in terms of $eU/k_B T$ arises because (1) the low-energy behavior of the DOS inside the bridge is dominated by one single infrared divergent process (in the present case diffusion modes coupling to the single-particle states via dynamically screened Coulomb interaction), which ensures that the DOS is described by a scale-independent function of the quasiparticle energy; (2) the low-energy cutoff, which determines the units of the dimensionless energies y and u , is the same in the reservoirs and in the interacting region. This means that the reservoir temperature T (entering through the distribution functions f^o in Eq. (6)) and the width of the Fermi steps in the bridge (entering through Eq. (3)) must be the same, i.e. energy relaxation in the bridge must be negligible; (3) a finite bias voltage is maintained between the leads. A high lead-to-bridge aspect ratio and a short nanobridge are essential to establish conditions (2) and (3) at the same time.

Finally, we can estimate the amplitude A of the Aronov-Al'tshuler conductance correction compared to

the background conductance $G(0, 1 \text{ K})$. Assuming that each channel contributes equally to the conductance, the unknown coupling constant Γ cancels in the ratio $r = A/G(0, 1 \text{ K})$. We obtain $r \approx 1.0 \cdot 10^{-4}$, which is in reasonably good agreement with the experimental result $r \simeq 2.6 \cdot 10^{-4}$ (see Fig. 2), considering the crudeness of the estimate.

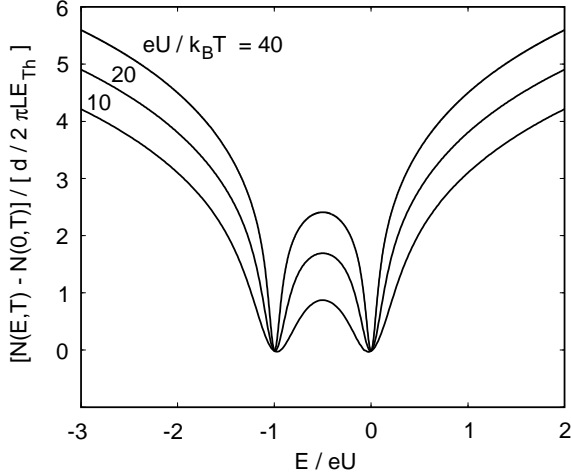


FIG. 6. The normalized DOS correction $\delta\mathcal{N}(E)$, Eq. (10), is shown for symmetric couplings $\Gamma^L = \Gamma^R$ at fixed temperature T for various values of the dimensionless voltage $eU/k_B T$.

Very recently, it has been proposed that logarithmic corrections to the conductance may also be caused by charge fluctuations between bridge and the reservoirs even in a clean system¹⁹. This correction can presumably be understood as the leading logarithmic behavior of an orthogonality catastrophe caused by the vanishing overlap between different charge states of the bridge. A similar effect has been considered by Matveev and Larkin²⁰ in the context of tunneling through a charged impurity. It remains to be seen whether this may provide an explanation of the ZBA in our samples.

IV. CONCLUSION

We have performed differential conductance measurements on small 2-dimensional metal bridges, whose Thouless energy is larger than the temperature. A controlled non-equilibrium situation was established by using a high aspect ratio between the lead and bridge thickness. We observe a ZBA with logarithmic scaling behavior as a function of the dimensionless bias voltage $eU/k_B T$. The observed scaling curve as well as the amplitude of the effect are in good quantitative agreement with our theoretical prediction that in short bridges ($E_{Th} > k_B T$) the Al'tshuler-Aronov DOS correction

shows $\ln\omega$ behavior instead of the $(\ln\omega)^2$ behavior of infinite films. For the observed scaling behavior to occur it is crucial that, despite the metallic contact to the leads, eigenstates in the bridge survive due to strong wave-function mismatch caused by the enormous lead-to-bridge aspect ratio.

We are grateful to A. Mirlin, H. Pothier, and B. L. Al'tshuler for useful discussions. This work was supported by DFG through SFB195.

[†] Present address: Forschungszentrum Karlsruhe, Institut für Nanotechnologie, D-76021 Karlsruhe, Germany.

E-mail: heiko.weber@int.fzk.de

- ¹ For a review see B.L. Al'tshuler and A.G. Aronov in *Electron-Electron interactions in Disordered Systems*, 1 (North-Holland, Amsterdam, 1985).
- ² B.L. Al'tshuler and A.G. Aronov, *Solid State Comm.* **30**, 115 (1979); B.L. Al'tshuler, A.G. Aronov and P.A. Lee, *Phys. Rev. Lett.* **44**, 1288 (1980).
- ³ Y. Imry and Z. Ovadyahu, *Phys. Rev. Lett.* **49**, 841 (1982).
- ⁴ G. Hertel, D.J. Bishop, E.G. Spencer and J.M. Rowell, *Phys. Rev. Lett.* **50**, 743 (1983).
- ⁵ I.O. Kulik and I.K. Yanson, *Sov. J. Low. Temp. Phys.* **4**, 596 (1978).
- ⁶ K. E. Nagaev, *Phys. Rev. B* **57**, 4628 (1998).
- ⁷ H. Pothier, S. Guéron, N.O. Birge, D. Estève and M.H. Devoret, *Phys. Rev. Lett.* **79**, 3490 (1997).
- ⁸ M. Henny, S. Oberholzer, C. Strunk, and C. Schönberger, *Phys. Rev. B* **59**, 2871 (1999).
- ⁹ For a comprehensive overview and references see D. L. Cox and A. Zawadowski, *Adv. Phys.* **47**, 599 (1998).
- ¹⁰ D. C. Ralph et al., *Phys. Rev. Lett.* **72**, 1064 (1994); D. C. Ralph and R. A. Buhrman, *Phys. Rev. B* **51**, 3554 (1995).
- ¹¹ Y. Meir and N.S. Wingreen, *Phys. Rev. Lett.* **68**, 2512 (1992).
- ¹² G. J. Dolan and J. H. Dunsmuir, *Physica B* **152**, 7 (1988).
- ¹³ S. Chakravarty and A. Schmid, *Phys. Rep.* **140**, 193 (1988).
- ¹⁴ M. H. Hettler, J. Kroha and S. Hershfield, *Phys. Rev. Lett.* **73**, 1967 (1994).
- ¹⁵ Yu. V. Nazarov, *Sov. Phys. JETP* **68**, 561 (1989).
- ¹⁶ C. Caroli, R. Combescot, P. Nozières and D. Saint-James, *J. Phys. C* **4**, 916 (1971).
- ¹⁷ A detailed derivation of the quasiclassical description of the non-equilibrium distribution function can be found in L. D. Landau and E. M. Lifshitz, *Course of Theoretical Physics*, Vol. 10, *Physical Kinetics*, Chapt. X (Butterworth-Heinemann, Oxford, 1997).
- ¹⁸ V. I. Kozub and A. M. Rudin, *Phys. Rev. B* **52**, 7853 (1995).
- ¹⁹ D. S. Golubev and A. D. Zaikin, *cond-mat/0010493* (2000).
- ²⁰ K. A. Matveev and A. I. Larkin, *Phys. Rev. B* **46**, 15337 (1992).